UNDERSTANDING WAVE ENERGY TRANSFORMATION THROUGH CONSTRUCTED OYSTER REEFS

Amy Bredes[1], Jon Miller[1], and Matt Janssen[1]

Wave attenuation datasets were collected from four constructed oyster reef (COR) fields sites across New Jersey and Connecticut. The sites span a diverse range of techniques used in practice including oyster castles, gabion baskets, and reef balls. All sites are submerged for part of or all of the tidal cycle to promote oyster recruitment. While submerged, wave amplification was observed at all four sites. COR are designed under the dual mandate of habitat creation and wave attenuation to reduce marsh edge erosion. However, the consensus in leading literature is marsh edge erosion is related to the energy flux, not wave height alone. Inspired by this and laboratory investigations of wave height amplification in the energy spectrum, the field data is analyzed to compare the transmission of wave height and energy flux through the COR. It was found that when wave heights were amplified, wave energy flux decreased 46% of the time. In the most extreme case, energy flux transmission showed a 48% reduction while wave height transmission showed a 135% increase. Under conventional design approaches using wave height transmission alone, the COR exhibiting wave amplification would be considered a design failure from the wave attenuation standpoint. This highlights the limitations of wave height transmission analysis in quantifying the performance of submerged shore protection structures. It is suggested that wave energy flux and wave energy flux transmission provides a more complete metric for design and evaluation of CORs.

Keywords: nature based solutions; living shorelines; wave attenuation; marsh edge erosion; energy flux

INTRODUCTION

Nature based solutions (NbS) are a classification of infrastructure that incorporates natural systems, both existing and created, and are increasingly being used in coastal protection systems (Bridges et al., 2022). One of the techniques gaining popularity is constructed oyster reefs (CORs). CORs are artificial structures that provide oyster spat a hard surface to colonize, and often in the context of coastal protection, are designed to attenuate wave energy (Wiberg et al., 2019). In order to provide the desired habitat for oysters, these structures must be submerged for most or all of the tidal cycle, depending on species and climate (Morris et al., 2019a), a departure from traditional emergent breakwater design. In the scheme of a larger coastal protection system, CORs are often used to reduce edge erosion of a salt marsh that is also being protected for its ecological and coastal protection services. Reducing erosion along the edge of the marsh is important, as acreage of marsh is reduced, so is protectiveness of the marsh. This becomes even more concerning as storm intensity increases and sea level rises (Sun and Carson, 2020).

Historically breakwater design has used a simplified approach, evaluating the reduction in wave height through the transmission coefficient (d'Angremond et al., 1996; van der Meer et al., 2005). This simplification is appropriate for traditional structures that are typically large and emergent. However, when designing a submerged structure where the objective is not only reducing wave energy but modifying wave shape, more complete metrics such as energy flux, which relates wave height and group velocity should be used. This approach can be seen in other types of coastal engineering design, such as in the design of surf reefs (Cáceres et al., 2010).

Marsh edge erosion is thought to be directly related to wave power, with multiple researchers fitting erosional data to wave power with experimentally fit coefficients based on field site conditions (Priestas et al., 2015; Schwimmer, 2001). Through a dimensional analysis, Marani et al. attempt to create an equation that describes erosional rate, using a theoretical framework considering vertical scarp elevation, water depth, mean wave power, and marsh cohesion, a value expressing the susceptibility of the soil to be removed by incident waves (Marani et al., 2011). While marsh cohesion, scarp elevation, and relative water depth can vary from marsh to marsh and even within the same marsh, mean wave power is the most important factor related to wave climate. Low marsh grass species tolerate certain wave conditions. Spartina alterniflora, the dominant species in the region in this study, is more tolerant of shorter-period waves (2–6 seconds) and prefers low to moderate wave energy conditions, with wave heights less than 0.3-0.5 meters (Halvorson and Singer, 1974; Roland and Douglass, 2005). In fact, Spartina alterniflora has been observed to attenuate wave energy across a range of frequencies, although it is particularly effective at dissipating higher-frequency waves (Zhang et al., 2020). These requirements are more easily evaluated using wave power rather than wave height. However, wave power is not the metric most engineering design is based on, instead wave height is used as a proxy for wave energy (d'Angremond et al., 1996; van der Meer et al., 2005).

[1] Davidson Laboratory, Stevens Institute of Technology, 1 Castle Point Terrace, Hoboken, NJ 07030, USA

From an engineering design perspective, wave attenuation of a breakwater, including CORs, is most dependent on relative freeboard and relative crest width, with the greatest wave attenuation when the crest of the structure is at or above still water level (Allen and Webb, 2011; Wiberg et al., 2019). This however, is at odds with the habitat constraints of most shellfish species, which require submergence the majority of the tidal cycle (Morris et al., 2019b). Artificial reefs constructed from crushed shell and oyster castles in Virginia, USA were found to reduce wave heights by an average of 30-50% for water depth of 0.5-1.0 m and 0-20% for water depths of 1.0-1.5 m with widths ranging from 0.5 to 5 m, wave height attenuation was reduced with water depth at these sites (Wiberg et al., 2019). Additionally, some field studies found wave heights were amplified in certain conditions, often when structures were submerged (Bredes et al., 2022; Wang et al., 2021). This is counter to the intention of these structures, reducing wave heights. However, when wave heights are amplified, is wave power similarly elevated?

The goal of this research is to understand the prevalence and mechanisms that lead to wave height amplification and understand if wave height amplification truly has negative implications for marsh edge erosion through the current understanding of the relationship between wave power and marsh edge erosion. By understanding wave impact to marshes through wave power, a greater understanding for effective COR design is achieved. To achieve these goals, gauges were deployed at four different COR sites that experience submergence and the changes in wave characteristics before and after the structures were assessed.

METHODS

Data was collected from four different constructed oyster reef field sites from 2021 through 2024 (Figure 1). The sites surveyed were located in Delaware Bay, NJ (Gandys Beach), Barnegat Bay, NJ (Forked River), Raritan Bay, NJ (Naval Weapon Station Earle), and Long Island Sound, CT (Stratford Point). These sites present a wide variety of submerged and semi-submerged structures meant to serve as constructed oyster reefs. Gandys Beach (Gandys) and Naval Weapon Station Earle (NWSE) have oyster castles deployed, the oyster castles at Gandys are in a single row and run cross shore along the eroding marsh and while mostly submerged, are emergent for a portion of the tidal cycle, while the oyster castles at NWSE are in several rows across a tidal flat and are submerged the entire tidal cycle. At Forked River (Forked) the CORs are steel gabion baskets filled with rock and seeded with spat that are submerged the entire tidal cycle as well. These gabion baskets are placed at angles in two rows running cross shore. Finally, Stratford Point (Stratford) is constructed with reef balls that are emergent for much of the tidal cycle, however become submerged for part of the tidal cycle, and are in a combination of single rows and double rows. All of the structures at these sites approach gradually sloping beaches or tidal flats with no harsh scarps on the inland area where gauge transects were deployed. Figure 1 shows images of the structures present at each site.

Figure 1. Images of the structures located all four sites, from the top left counterclockwise, Gandys Beach oyster castles, Forked River gabion baskets, Stratford Point reef balls, and Naval Weapon Station Earle oyster castles.

At each site, wave data was collected with pressure gauges (RBR solo^3) and locations of gauges and structures were measured using RTK-GPS to collect elevations, locations, and dimensions of structures and gauges. Gauges were placed 2-3 meters in front and behind the structures at each field site. Data collected from these gauges was then spectrally processed using the WAFO package (Brodtkorb et al., 2000). Using the moments and frequencies, zero moment wave heights (H_{m0}), and peak periods (T_p) were calculated directly from field data. Subsequently, a variety of parameters were calculated to assess and compare the wave attenuation at these sites using linear wave theory. Several calculations were completed for each gauge. Relative freeboard (F/H_{m0}) and freeboard to depth ratio (F/d) were calculated. Wavelength (L) was calculated iteratively using linear wave theory:

$$L = \frac{gT^2}{2\pi}\tanh\left(\frac{2\pi d}{L}\right) \quad (1)$$

where T is period, gravity (g) is 9.81 m/s^2, L is wavelength, and d is water depth. From this calculation, Ursell number (Ur),

$$Ur = \frac{H_{m0}L^2}{d^3} \quad (2)$$

wave steepness (S),

$$S = \frac{H_{m0}}{L} \quad (3)$$

celerity (c),

$$c = \frac{gT}{2\pi}\tanh\,(kd) \quad (4)$$

group velocity (c_g),

$$c_g = \frac{1}{2}c_p\left(1 + \frac{2kd}{\sinh(2kd)}\right) \quad (5)$$

wave energy flux, also known as wave power (P), and wave energy (E) were calculated:

$$P_w = \frac{c_g \rho g H_{mo}^2}{8} = c_g E \quad (6)$$

where k is wave number, and ρ is water density. Subsequently, several calculations were completed to compare the inshore and offshore gauges at these sites. In order to understand how the structures impacted waves as they pass through the CORs, transmission coefficient (Kt) was calculated,

$$K_t = \frac{H_{m0t}}{H_{m0i}} \quad (7)$$

where the subscripts t and i indicate transmitted conditions and incident conditions, respectively. Given the relationship between wave power, a function of both wave height and group velocity, and marsh edge erosion; a new parameter, power transmission coefficient (Pt), was calculated. Power transmission coefficient is similar to transmission coefficient, however instead of a ratio of wave heights, it is a ratio of wave energy flux on either side of the structure:

$$P_t = \frac{P_{wt}}{P_{wi}} \quad (8)$$

where Pwt is the transmitted wave power and Pwi is the incident wave power. Field data was filtered to remove less accurate pressure readings by removing measurements below 5 cm. Additionally, to ensure the validity of the use of linear wave theory, measurements with a calculated Ursell number below 100 were excluded.

RESULTS

Sites were characterized through the structure dimensions and wave climate data collected. Table 1 shows the average incident wave heights, period, and wavelength, as well as the dimensions, freeboards, and depths of the structures. Observations at the sites had similar mean incident wave heights, however period and wavelength varied more greatly between the sites.

Table 1. Mean site characteristics for all sites surveyed.

	Hm0	Tp	L	% sub. obs.	FH	Crest depth	Structure depth
Stratford Double Row	0.18	31.7	104	9%	1.2	0.47	-0.58
Stratford Single Row	0.18	31.5	102	10%	0.8	0.34	-0.66
NWSE	0.18	7.9	30.1	100%	-10.4	-1.36	-1.5
Forked	0.18	2.7	8.9	100%	-2.4	0.07	-0.66
Gandys 2021	0.21	7.9	25.3	60%	-1.1	-0.68	-1.41
Gandys 2024	0.17	9.2	38.1	85%	-6.3	-0.68	-1.41

Notes: Hm0 = incident wave height in meters, Tp = peak period in seconds, L = wave length in meters, % sub. obs. = percentage of submerged observations, FH = relative freeboard (non dimensional), crest depth and structure depth are in meters

Wave Heights

Wave height amplification was observed at all four sites studied, highlighted in the shaded boxes in Figure 2. Additionally, trends were observed in wave transmission and submergence. Forked and NWSE, the two sites submerged the majority of the time, showed the majority of transmission coefficients of near 1, indicating no impact on wave heights, for the majority of the observations. This is not unexpected given the documented relationship between relative freeboard and wave height transmission coefficient (d'Angremond et al., 1996; Seabrook and Hall, 1998; van der Meer et al., 2005). Both of these sites experience relatively small wave heights in fetch limited locations. The transmission coefficients at Statford and Gandys show a bimodal distribution with peaks around 1 and around 0.1. This bimodal distribution is likely due to the changes in the tidal cycle. The two observations at Gandys, one from 2021 and 2024 are likely different due to difference in storm intensity during the deployments.

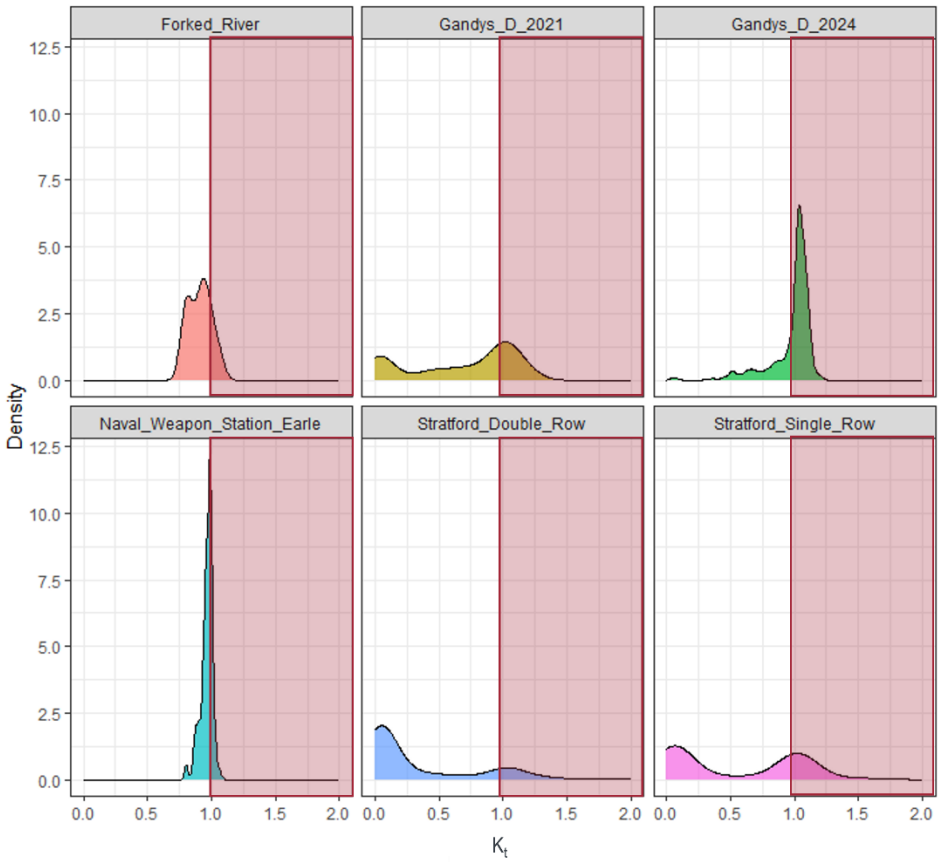

Figure 2. This figure includes all data collected and analyzed at all four field sites, including two different deployments at Gandys and the single and double rows at Stratford. In the red boxes, incidents of wave height amplification (Kt > 1) are highlighted, with the x-axis showing transmission coefficient and the y-axis showing the density of the observation. Amplification was observed at all field sites.

The expected relationship between transmission coefficient and relative freeboard is also seen in the bulk data (Figure 3). Similar in the relationship identified by many existing formulas, relative freeboard has a strong relationship with wave transmission, as mentioned above. When relative freeboard indicates emergence (in Figure 3, x-axis below 0), minimal wave transmission occurs and the majority of waves are almost completely attenuated, with transmission coefficients largely below 0.2. When relative freeboard indicates submergence (in Figure 3, x-axis above 0), wave heights are being minimally impacted by the structure, with transmission coefficients hovering around 1. Between the submerged and emerged conditions, observations can be seen with a wide variety of transmission coefficients. It is expected for transmission coefficient to form a curve between the submerged and emerged conditions, as indicated by the line in Figure 3. The large spread in the data is reflective of the different designs and field conditions between sites, as well as the expected variance from field data collection.

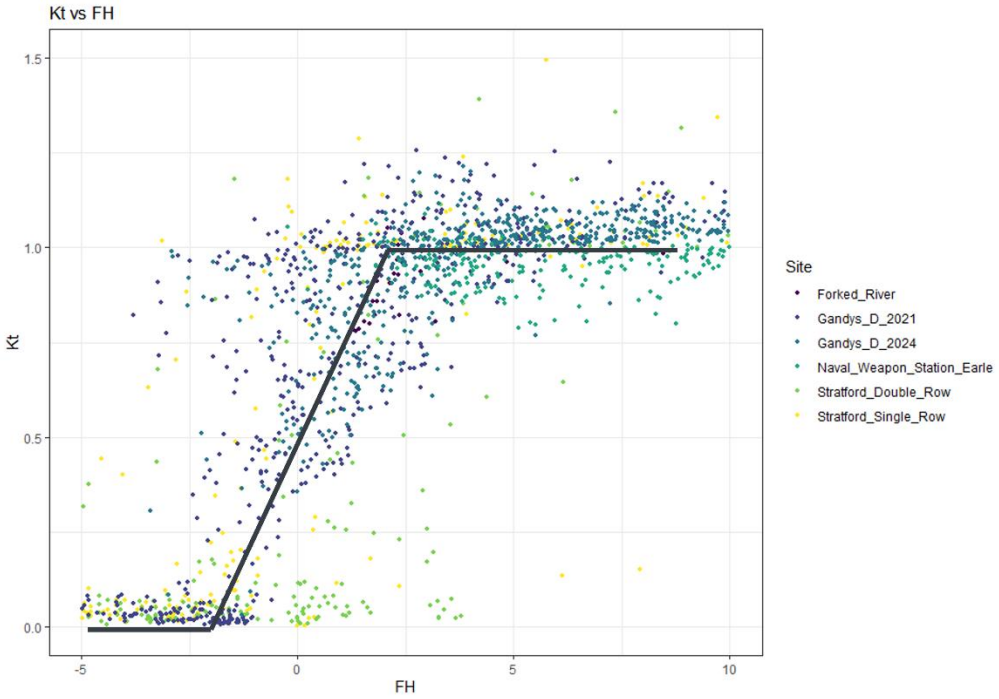

Figure 3. Transmission coefficient (Kt) vs relative freeboard (FH) of all sites, where submerged conditions are displayed as positive and emergent conditions are shown as negative.

Energy Flux

Energy flux and subsequently, wave power transmission coefficient was calculated for the same filtered observations that wave height transmission coefficient was calculated with (Figure 4). Overall, average Pt for all sites was 0.66 while average Kt for all sites was 0.76. Even more importantly, when wave height amplification occurred, average Pt and Kt over all sites were 0.84 and 1.05, respectively. During submerged conditions, some of the sites, the Stratford Single Row and Gandys 2024 experienced wave height amplification, while still experiencing a reduction in wave energy flux. When comparing Kt and Pt among the sites, the largest difference during wave height amplification was seen at the Stratford Double Row site, with average Pt and Kt of 0.66 and 1.11. The means for all of the sites can be seen in Table 2.

Wave power transmission coefficient was also plotted against relative freeboard in Figure 5. While the data follows a similar pattern, the observations are more dense when Pt is 0 and there is a higher density of observations in the intermediate relative freeboard values between the submergent and emergent conditions than when assessing the same trends with wave height transmission coefficient.

Table 2. Average Pt and Kt for all of sites surveyed during all conditions, during wave height amplification, and during structure submergence

	Mean - all		Mean – Kt > 1		Mean - Submerged	
	Kt	Pt	Kt	Pt	Kt	Pt
Stratford Double Row	0.30	0.14	1.11	0.66	0.72	0.50
Stratford Single Row	0.50	0.33	1.04	0.79	1.06	0.89
NWSE	0.96	0.93	1.02	1.01	0.96	0.93
Forked	0.91	0.80	1.04	1.04	0.91	0.80
Gandys 2021	0.64	0.50	1.06	0.98	0.97	0.86
Gandys 2024	0.97	0.89	1.06	1.03	1.02	0.97

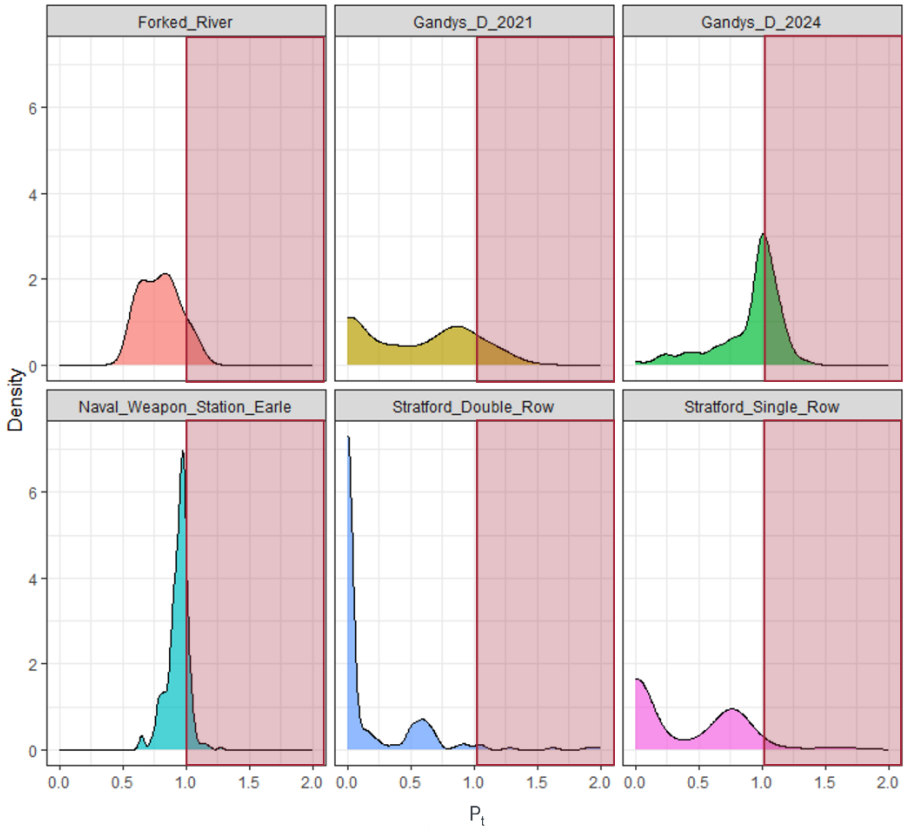

Figure 4. This figure includes all data collected and analyzed at all four field sites, including two different deployments at Gandys and the single and double rows at Stratford. In the red boxes, incidents of wave power increases (Pt > 1) are highlighted, with the x-axis showing power transmission coefficient and the y-axis showing the density of the observation. These incidents over 1 are likely a result of processes such as diffraction and reflection.

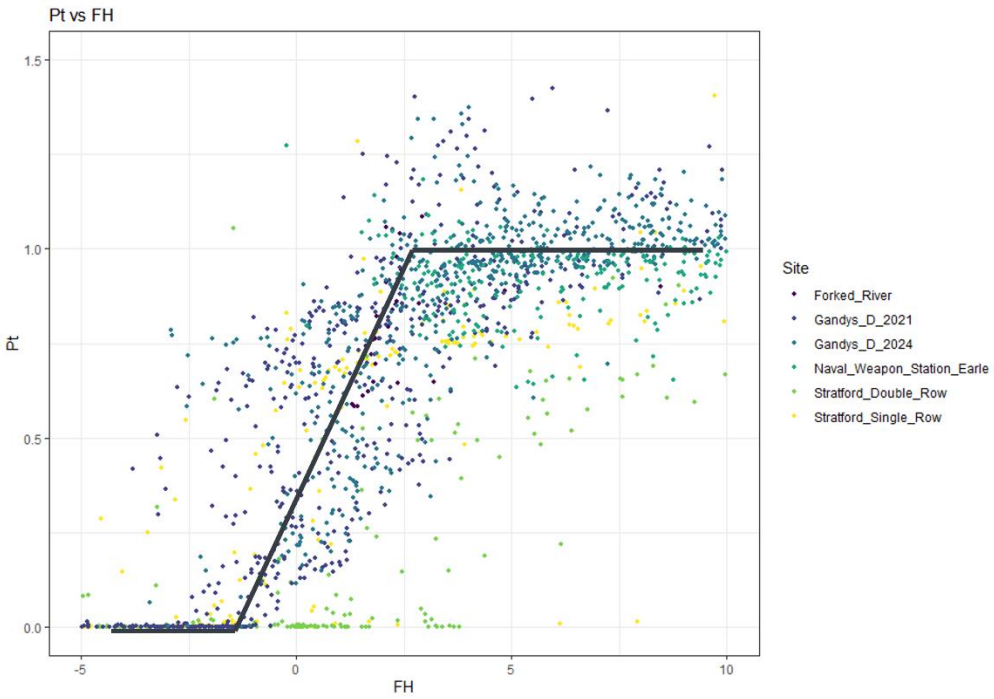

Figure 5. Power transmission coefficient (Pt) vs relative freeboard (FH) of all sites, where submerged conditions are displayed as positive and emergent conditions are shown as negative.

DISCUSSION

The observations of amplification at all sites shows that the two previously documented observations of wave height amplification by submerged CORs at the same field site, Gandys, were not novel occurrences (Bredes et al., 2022; Wang et al., 2021). While these observations are novel in the field, they have been documented in laboratory testing. Testing has shown that the wave profile evolving over and past a breakwater can undergo significant steepening and nonlinear amplification as it passes over the breakwater, with maximum crest elevation increasing by as much as 25% (Christou et al., 2008). This is similar to the degree of amplification seen in this study. However, it was found that while there were still instances of Pt exceedances over 1, there were much fewer, and overall, the average wave the density of the distributions shifted left (Figure 4). In Table 2, wave power transmission coefficient was less than wave height transmission coefficient for all conditions. This is largely due to wave power being a function of both wave height and group velocity.

Group velocity decreased as waves traveled inshore, with offshore observations consistently greater than inshore observations (Figure 5). At the more submerged sites the difference between the inshore and offshore group velocity was less, likely due to the flatter bathymetry at these sites. Additionally, as waves move inshore and group velocities decrease below 2 m/s, the waves are likely becoming more cnoidal, increasing scatter. These changes in group velocity are evidence that shoaling is occurring at these sites, likely contributing to the observations of amplified wave heights.

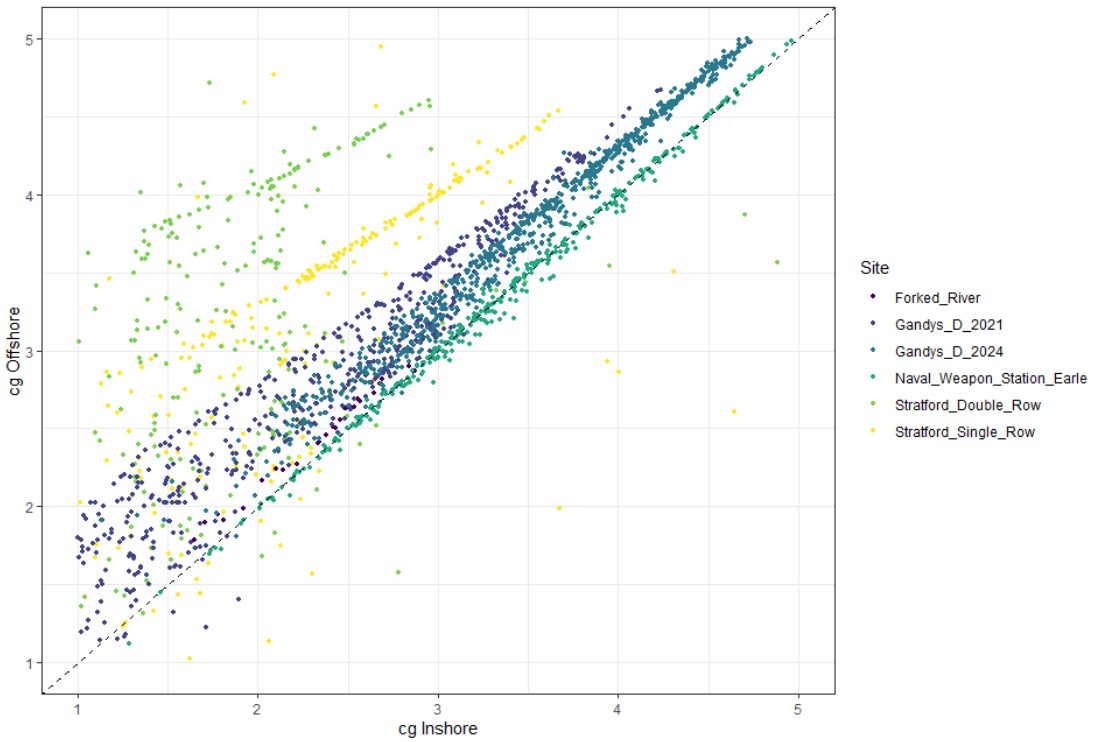

Figure 6. Group velocity difference between inshore and offshore of all structures. Group velocity is consistently reduced as waves move inshore.

To isolate the impact of the structure on waves and determine what wave height and group velocity changes are from shoaling, group velocity and wave height were estimated using the dispersion relationship to estimate the wave behavior in absence of CORs (Figure 7). In Figure 7, there are several distinct regimes describing wave-structure interactions; clear dramatic wave reductions in the vertical portion where measured values are near 0 and structures are emergent, the triangle above the 45 degree line where there is effective wave height reduction, an area around the 45 degree line where the structures have no impact on wave heights, and finally and amplification zone below the line. On average for all data, regardless of submergence, group velocity and wave height varied 5% and 50%, respectively, between calculated and measured values. When structures were submerged, group velocity and wave height on average varied 2% and 18%, respectively, between calculated and measured values. However, for instances of wave amplification (Kt > 1), group velocity and wave

height varied by 2% and 9% on average between the calculated and measured. Unsurprisingly, the wave heights are impacted more by the structures, however, group velocity is still impacted by structures, independent of expected changes from the shoaling process. When comparing sites, group velocity was most impacted at Stratford (reef balls) with a 9% average difference between the calculated and measured values.

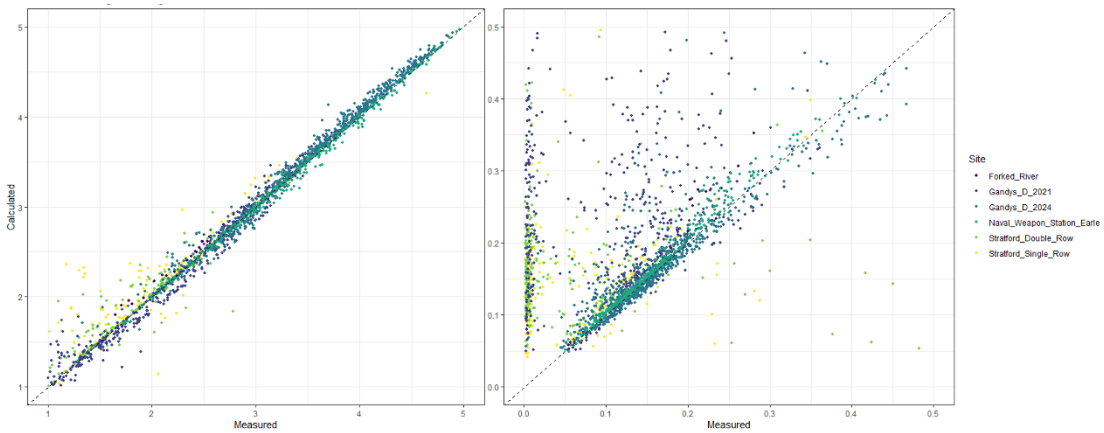

Figure 7. Estimations were calculated using the inshore depths to approximate the expected wave height and group velocity as a result of shoaling (x-axis) and compared to the field measurements (y-axis), group velocity and wave height are shown on the left and right, respectively.

Pt and Kt were plotted against each other to further visualize the difference between the parameters. Figure 8 can be separated into three regimes; regime A where Pt is less than Kt, but both indicate dissipation, regime B where Kt indicates amplification, but Pt indicates dissipation, and regime C where Pt is greater than 1. While power transmission should never exceed 1 due to the conservation of energy, these observations indicate an additional energy source. This is likely related to diffraction and reflection at the site. To explore the energy contributions at the site an energy balance was developed:

$$E_t + E_r + E_{diss} = E_i + E_{diff} + E_r \quad (9)$$

where E_t is the transmitted energy, E_r is the energy reflected off the structure, E_{diss} is the energy dissipated by the structure, E_i is the incident energy, E_{diff} is the additional energy from diffraction, and E_r is the energy reflected from the beach. For the analysis completed in this paper, a simplified 1D model was assumed, where diffraction, and reflection were neglected. During field data collection, arrays were not deployed, creating limitations to the ability to isolate these components. However, future work aims to isolate the dissipation caused by structures and separated the diffraction and reflection components.

Due to the squared wave height component, wave power transmission coefficient is negligible when wave height transmission coefficient is below 0.25. Additionally, the influence of group velocity reduces wave height amplification results; when wave heights were amplified, wave energy flux decreased due to changes in group velocity. In the most extreme case, energy flux transmission showed a 48% reduction when wave height transmission coefficient showed a 135% amplification. This points the bias created by wave height driven goals in nature based design of constructed oyster reefs. Others have noted the incongruence between the desire for oyster based coastal protection and the mismatch between the biologic needs of oyster species (i.e. large footprints with frequent submergence) with current engineering design practices (i.e. narrow and emergent) (Morris et al., 2019b).

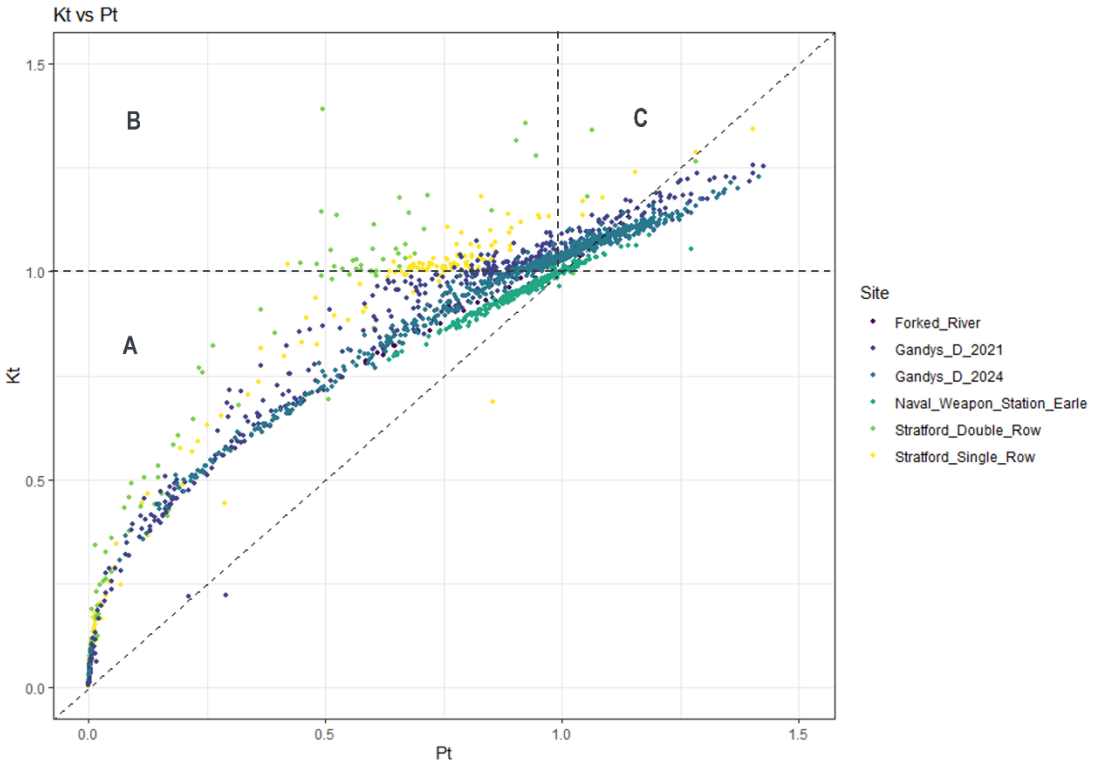

Figure 8. A plot of all sites with transmission coefficient (Kt) vs energy flux transmission coefficient (Pt). This plot is divided into the three regimes; A, where Kt and Pt both show attenuation but, Kt is greater than Pt, B, where Kt indicates amplification, but Pt indicates dissipation, and C, where Pt is greater than 1. The "amplification" events in regime C, however these events are likely due to diffraction, reflection, and other components adding energy not recorded on the offshore gauge.

CONCLUSIONS

Wave amplification has been noted at all sites and is closely associated with relative freeboard conditions. Despite wave amplification, these sites see a reduction in inshore energy flux. This suggests the structure influences incident wave conditions through shoaling processes with the influence of the structure and the reduction in energy flux attributed to dissipation and reflection. Quantifying COR influence on the respective reflection and dissipation components is an area of future research; particularly at the Gandys Beach site.

Evaluating wave height transmission and ignoring the entire wave transformation by structures is leaving out important information that should dictate design. Wave energy flux transmission should be considered as it better represents the complexity of wave transformation over and through structures, allowing for more robust and thoughtful design. The flaws of only evaluating wave height when designing structures are evident by wave height amplification observations still correlating to a reduction in total wave energy flux.

FUTURE WORK

To continue enhancing the understanding of the field data collected in this study, an energy balance and further understanding of the energy contributions into the transmitted waves need to be assessed to remove events of amplification associated with measurement, not with actual wave height amplification. Understanding how to use a combination of wave power transmission and water level along the marsh edge to inform effective design of marsh edge protection is needed. This field work is also limited by the structures that have been constructed. Larger width structures are currently of interest for more effective attenuation when submerged and more research needs to be done in this area to further improve COR construction and design.

ACKNOWLEDGMENTS

This research was supported in part by funding from the US Coastal Research Program (USCRP) under grant #W912HZ2220007.

REFERENCES

Allen, R.J., and B.M. Webb, 2011. Determination of wave transmission coefficients for oyster shell bag breakwaters, Proceedings of the Coastal Engineering Practice 2011. San Diego, CA.

Bredes, A.L., Miller, J.K., Kerr, L., and D.R. Brown, 2022. Observations of Wave Height Amplification Behind an Oyster Castle Breakwater System in a High-Energy Environment: Gandys Beach, NJ. Front. Built Environ. 8, 884795. https://doi.org/10.3389/fbuil.2022.884795

Bridges, T.S., Smith, J.M., King, J.K., Simm, J.D., Dillard, M., deVries, J., Reed, D., Piercy, C.D., van Zanten, B., Arkema, K., Swannack, T., de Looff, H., Lodder, Q., Jeuken, C., Ponte, N., Gailani, J.Z., Whitfield, P., Murphy, E., Lowe, R.J., McLeod, E., Altman, S., Cairns, C., Suedel, B.C., and L.A. Naylor, 2022. Coastal Natural and Nature-Based Features: International Guidelines for Flood Risk Management. Front. Built Environ. 8, 904483. https://doi.org/10.3389/fbuil.2022.904483

Brodtkorb, P.A., Johnannesson, P., Lindgren, G., Rychlik, I., Rydén, J., and E. Sö, 2000. WAFO - a Matlab toolbox for analysis of random waves and loads. Proc 10th Int Offshore Polar Eng Conf III, 343–350.

Cáceres, I., Trung, L.H., Dirk Van Ettinger, H., Reniers, A., and W. Uijttewaal, 2010. Wave and Flow Response to an Artificial Surf Reef: Laboratory Measurements. J. Hydraul. Eng. 136, 299–310. https://doi.org/10.1061/(ASCE)HY.1943-7900.0000177

Christou, M., Swan, C., and O.T. Gudmestad, 2008. The interaction of surface water waves with submerged breakwaters. Coast. Eng. 55, 945–958. https://doi.org/10.1016/j.coastaleng.2008.02.014

d'Angremond, K., Van Der Meer, J.W., and R.J. De Jong, 1996. Wave Transmission at Low-Crested Structures, in: Coastal Engineering. Presented at the 25th International Conference on Coastal Engineering, American Society of Civil Engineers, Orlando, Florida, United States, pp. 2418–2427. https://doi.org/10.1061/9780784402429.187

Halvorson, W.L., and A.C. Singer, 1974. Growth Responses of Spartina patens and Spartina alterniflora Analyzed by Means of a Two-Dimensional Factorial Design. Am. Midl. Nat. 91, 444. https://doi.org/10.2307/2424336

Marani, M., D'Alpaos, A., Lanzoni, S., and M. Santalucia, 2011. Understanding and predicting wave erosion of marsh edges: MARSH EDGE EROSION. Geophys. Res. Lett. 38, n/a-n/a. https://doi.org/10.1029/2011GL048995

Morris, R.L., Bilkovic, D.M., Boswell, M.K., Bushek, D., Cebrian, J., Goff, J., Kibler, K.M., La Peyre, M.K., McClenachan, G., Moody, J., Sacks, P., Shinn, J.P., Sparks, E.L., Temple, N.A., Walters, L.J., Webb, B.M., and S.E. Swearer, 2019a. The application of oyster reefs in shoreline protection: Are we over-engineering for an ecosystem engineer? J. Appl. Ecol. 56, 1703–1711. https://doi.org/10.1111/1365-2664.13390

Priestas, A., Mariotti, G., Leonardi, N., and S. Fagherazzi, 2015. Coupled Wave Energy and Erosion Dynamics along a Salt Marsh Boundary, Hog Island Bay, Virginia, USA. J. Mar. Sci. Eng. 3, 1041–1065. https://doi.org/10.3390/jmse3031041

Roland, R.M., and S.L. Douglass, 2005. Estimating Wave Tolerance of Spartina alterniflora in Coastal Alabama. J. Coast. Res. 213, 453–463. https://doi.org/10.2112/03-0079.1

Schwimmer, R.A., 2001. Rates and Processes of Marsh Shoreline Erosion in Rehoboth Bay, Delaware, USA. J. Coast. Res. 17, 672–683.

Seabrook, S.R., and K.R. Hall, 1998. Wave Transmission at Submerged Rubblemound Breakwaters. Coast. Eng. Proc. 1.

Sun, F., and R.T. Carson, 2020. Coastal wetlands reduce property damage during tropical cyclones. Proc. Natl. Acad. Sci. 117, 5719–5725. https://doi.org/10.1073/pnas.1915169117

van der Meer, J.W., Briganti, R., Zanuttigh, B., and B. Wang, 2005. Wave transmission and reflection at low-crested structures: Design formulae, oblique wave attack and spectral change. Coast. Eng. 52, 915–929. https://doi.org/10.1016/j.coastaleng.2005.09.005

Wang, H., Capurso, W., Chen, Q., Zhu, L., Niemoczynski, L., and G. Snedden, 2021. Assessment of Wave Attenuation, Current Patterns, and Sediment Deposition and Erosion During Winter Storms by Living Shoreline Structures in Gandys Beach, New Jersey. US Geol. Surv.

Wiberg, P.L., Taube, S.R., Ferguson, A.E., Kremer, M.R., and M.A. Reidenbach, 2019. Wave Attenuation by Oyster Reefs in Shallow Coastal Bays. Estuaries Coasts 42, 331–347. https://doi.org/10.1007/s12237-018-0463-y

Zhang, X., Lin, P., Gong, Z., Li, B., and X. Chen, 2020. Wave Attenuation by Spartina alterniflora under Macro-Tidal and Storm Surge Conditions. Wetlands 40, 2151–2162. https://doi.org/10.1007/s13157-020-01346-w